How to cite: *Angew. Chem. Int. Ed.* **2021**, *60*, 25832–25838
International Edition: doi.org/10.1002/anie.202106881
German Edition: doi.org/10.1002/ange.202106881

Conformational Analysis

Noncovalent CH–π and π–π Interactions in Phosphoramidite Palladium(II) Complexes with Strong Conformational Preference

*Matej Žabka, Lavakumar Naviri, and Ruth M. Gschwind**

Abstract: *The weak noncovalent interactions and flexibility of ligands play a key role in enantioselective metal-catalyzed reactions. In transition metal complexes and their catalytic applications, the experimental assessment and the design of key interactions is as difficult as the prediction of the enantioselectivities, especially for flexible, privileged ligands such as chiral phosphoramidites. Therefore, the interligand interactions in cis-$Pd^{II}L_2Cl_2$ phosphoramidite complexes were investigated by NMR spectroscopy and computations. We were able to induce a strong conformational preference by breaking the symmetry of the C_2-symmetric side chain of one of the ligands, and shift the equilibrium between hetero- and homocomplexes towards heterocomplexes because of interligand interactions in the cis-complexes. The modulation of aryl substituents was exploited, along with the solvent effect. The combined CH–π and π–π interactions reveal design patterns for binding and folding of chiral ligands and catalysts.*

Introduction

Noncovalent, weak dispersive interactions are manifested throughout well-established structures in supramolecular chemistry, biology, and catalysis.[1] When combined, such interactions provide substantial stabilization of supramolecular host–guest complexes, aid in folding of extended molecules, enhance the binding of a catalyst with a substrate, or stabilize one diastereomeric transition state with a chiral reagent or a catalyst more than the other state(s). Currently, an extensive effort is devoted to designing dispersive interacting sites in molecules to exploit the elements essential for controlling conformation, binding, and reactivity in a predictable way in the area of asymmetric organocatalysis.[2–8] Moreover, quantification of weak interactions in terms of energy is highly desirable for the design of remarkably effective catalysts. Among such interactions, those involving aromatic rings (notably π–π and CH–π) have been studied in great detail using physical organic chemistry approaches, including molecular balances, thermodynamic double-mutant cycles, evaluation of solvent effects, and computational methods.[9–14] Recently, such interactions were also analyzed in protein–ligand complexes by NMR.[15] However, the systematic application of these concepts in transition metal catalysis is still rare,[16,17] and a suitable, realistic model that can aid in assessment and quantification of the interactions is sought. One approach is data-driven and utilizes multivariate regression analysis.[18] Ideally, the single experimental model should consider only the interligand interactions, be independent of any substrate, and thus be applicable to more complex systems.

Chiral phosphoramidite ligands are one of the most versatile and privileged ligands in asymmetric transition metal (TM) catalysis.[19,20] These ligands, based on binaphthyl or biphenyl backbone, were developed mainly by the groups of Feringa and Alexakis.[21–26] The aryl backbone, in combination with a highly flexible, usually C_2-symmetric amine side chain, provide multiple dispersion energy donor sites. The success of these ligands in a range of stereoselective transformations, and their broad substrate scope is attributed mainly to their flexibility and easily assembled modular structure, compatible with many transition metals. We previously suggested that the intermolecular interactions of phosphoramidite ligands are independent of the complexes they are active within. Specifically, we showed that the aggregation as a probe for intermolecular interaction is independent of the transition metal used, the complex composition (number of ligands) and even the structure as long as phosphoramidite ligands (of the basic structure used in the study) are involved.[27] This previous study allows us to choose the best NMR model for investigations and to claim at the same time that these interactions should be transferable to catalytic systems. Moreover, we first proposed the importance of the extended interaction areas between phosphoramidite ligands as the source of stereoselectivity in TM catalysis.[27,28] Following this report, interactions between the ligand and the substrates or ligands and metal (cation–π) have been proposed to be responsible for the high stereoinduction observed in many metal-catalyzed reactions.[29–31]

A few years ago we introduced a supramolecular balance based on bis(phosphoramidite) palladium(II) complexes, which provided the principal idea how to assess the noncovalent interactions between two ligands in TM complexes.[28,32] However, later examination of the balance by computational methods and detailed chemical shift analysis revealed a conformational exchange of an amine side chain in one of the complexes, not interpreted by the previous qualitative analysis, thus reducing the accuracy of the balance.

[*] Dr. M. Žabka, L. Naviri, Prof. Dr. R. M. Gschwind
Institute of Organic Chemistry
Universität Regensburg
Universitätstrasse 31, 93053 Regensburg (Germany)
E-mail: ruth.gschwind@chemie.uni-regensburg.de
Supporting information and the ORCID identification number(s) for the author(s) of this article can be found under: https://doi.org/10.1002/anie.202106881.

Therefore, in this work we present complexes with limited conformational flexibility that allow the application of the complexes in the balance to experimentally measure interligand interactions, the analysis of the interaction area and the design of ligands for high heterocomplex preferences. Such heterocomplexes can be useful in synthetic chemistry, because they can display increased activity or selectivity in metal-catalyzed reactions, especially in rhodium-catalyzed hydrogenations and conjugate additions.[33–39] On the other hand, palladium phosphoramidite complexes catalyze challenging allylic substitutions and domino-Heck reactions, and mechanistic insight would be welcome.[19,40–42] In addition, the experimental data about the relative energetics of these complexes allowed us to select and validate a suitable computational method, which could be potentially applied in the design of other TM systems.

Results and Discussion

To evaluate the heterocomplex preferences based on supramolecular interactions and their energetics using the supramolecular balance, the *cis*-complexes PdL_2Cl_2 were required. Initially, mixing the ligands and $Pd(cod)Cl_2$ (2:1) in nonpolar solvent CD_2Cl_2 gave *trans*-complexes PdL_2Cl_2.[43,44] Subsequently, these *trans*-complexes underwent slow isomerization to *cis*-isomers, stabilized by noncovalent interactions between the ligands in the *cis*-complexes (Figure 1 A). As shown in Figure 1 B, when using two different ligands, (*R*,*R*)-**A1** (Alexakis' flexible biphenol-based ligand) and (S_a,*R*,*R*)-**F** (Feringa's binaphthyl ligand), an equilibrium is established between heterocomplex *cis*-Pd(**A1**)(**F**)Cl_2 and the corresponding homocomplexes *cis*-Pd(**A1**)$_2Cl_2$ and *cis*-Pd(**F**)$_2Cl_2$. Separately, using an enantiomeric ligand **A1′**, another equilibrium consisting of a diastereomeric heterocomplex *cis*-Pd(**A1′**)(**F**)Cl_2 was established. By analyzing the $\Delta\Delta G$ between the two equilibria, we were able to quantify the difference of the noncovalent interaction energies between the diastereomeric complexes assuming that the Gibbs energies are the same for the enantiomeric homocomplexes *cis*-Pd(**A1** or **A1′**)$_2Cl_2$. In addition, the two homo-heterocomplex equilibria used in the balance provide direct access to ligand driven preferences of heterocomplex formation.

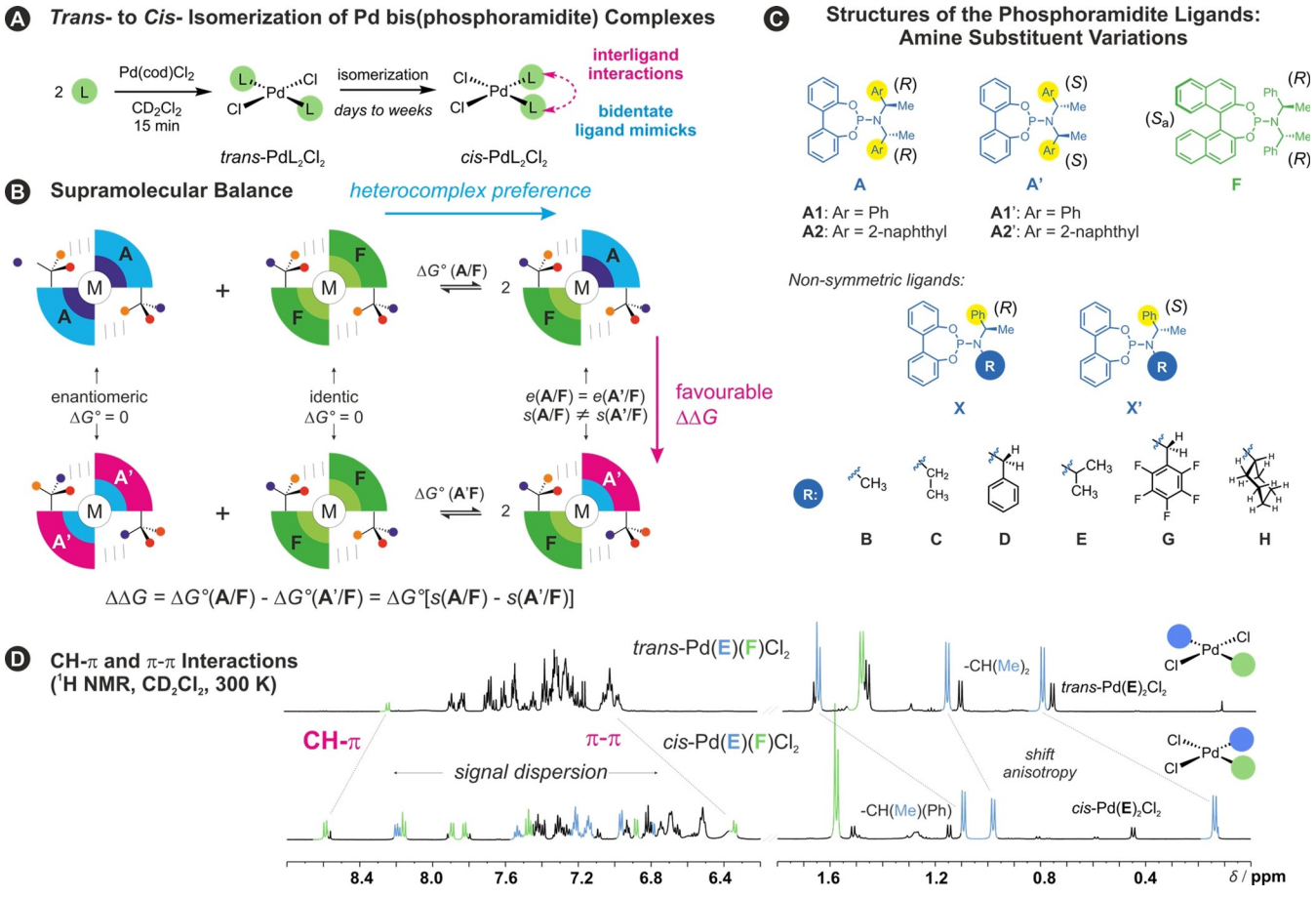

Figure 1. a) *cis*-Pd^{II} bis(phosphoramidite) complexes as model system for interligand interactions. b) Supramolecular balance: experimental access to the interaction difference between two diastereomeric heterocomplexes using the ligand combination **A**, **A′**, and **F**; for details see ref. [32]. c) Structures of the ligands used in the homo- and heterocomplex equilibria including alkyl group structural variations of the biphenyl phosphoramidite ligands **A** and **A′**. d) Tight interligand interactions in the *cis*-complexes manifested by significant chemical shift changes in the ^{1}H NMR spectra of *trans*- and *cis*-Pd(**E**)(**F**)Cl_2, as well as a large chemical shift dispersion in *cis*-Pd(**E**)(**F**)Cl_2 (CD_2Cl_2, 300 K).

From Flexibility to Conformational Preference

Since the previous report, we have found by a computational study that the heterocomplex *cis*-Pd(**A1′**)(**F**)Cl_2 is not conformational stable. One arm of the two amine side-chains of ligand **A1′** shows several interconverting conformers affecting the values of this complex in the above-mentioned supramolecular balance (see SI Chapter 12.5.6). To fix this issue, we set out to break symmetry of the flexible **A1** ligand's side chain that would reduce this conformational flexibility.

We thus modified one of the 1-phenylethyl groups (see Figure 1C and SI Chapter 4 for all structures) and designed ligands **X** containing various alkyl side chains with variable size, dispersion areas, and electronic properties such as methyl (**B**), ethyl (**C**), benzyl (**D**), isopropyl (**E**), pentafluorobenzyl (**G**), and cyclohexyl (**H**) groups. Equilibria containing ligands **B**, **C**, **D**, and **G** with ligand **F** showed more or less statistical distribution of the hetero- and homocomplexes based on ^{31}P NMR spectra (ratios around 2:1:1, Table 1). In addition, exchange crosspeaks were often found between various conformers in the NOESY spectra at 300 K suggesting considerable flexibility. In contrast, by introducing larger, branched isopropyl or cyclohexyl groups (the complexes containing ligands **E** and **H**), we indeed achieved conformational stability. Even variable-temperature (VT) NMR experiments from 300 K–180 K of heterocomplexes containing *cis*-Pd(**E** or **E′**)(**F**)Cl_2 did not reveal new peaks in ^1H or ^{31}P spectra confirming the high conformational stability of these *cis*-complexes.

The conformational stabilization seems to be connected to an increased preference for the heterocomplex. Thus, for ligands **E** and **H**, the equilibria were shifted towards the heterocomplexes even with ratios up to 8:1:1 for the **E** ligand and 22:1:1 for the **E′** ligand (Table 1). The combination of ligand **F** with a dynamic, achiral ligand **I** also showed a high heterocomplex ratio, suggesting that combinations with achiral ligands are suitable (see SI Chapter 6.2).

We subsequently analyzed the key interaction areas resulting in the heterocomplex preferences. In all *cis*-complexes, the emergence of noncovalent interactions is clearly manifested in ^1H NMR spectra: in the *trans*-complex, there is severe chemical shift overlap in the aromatic region, whereas in the *cis*-complex the signals are nicely dispersed over 2.4 ppm range (Figure 1D). Downfield shifts of the aromatic signals and upfield shifts of the methyl groups ($\Delta\delta$ −0.6 ppm) are attributed to the CH–π interactions, while the upfield shift of the aromatic signals are ascribed to π–π interactions. Since this trend is general for all complexes and not directly connected to heterocomplex preferences, we selected the complexes containing ligands **E** or **E′** for further structural studies.

In 1D and 2D NOESY spectra at 300 K exclusively interligand NOE contacts were observed between methyl and CH protons of (*R*)-Ph(Me)CH group and protons 3, 4, and 5 of the binaphthyl in **F** part of *cis*-Pd(**E**)(**F**)Cl_2 (red circle in Figure 2A and NOEs in Figure 2B), which confirms that the extended interaction area is responsible for the heterocomplex preference. In addition, only the intraligand contacts in both ligands (blue and green arrows in Figure 2A) were present, suggesting a major conformational preference even at 300 K. Identical NOE contacts in the NOESY spectra at 200–220 K confirmed this unexpectedly high stability. For the heterocomplex *cis*-Pd(**E′**)(**F**)Cl_2, a similar situation was encountered, and mostly interligand interaction of the phenyl ring (*S*)-Ph(Me)CH group of **E′** with binaphthyl was observed. This finding suggests that the Ph(Me)CH group remains oriented inside the complex forming the noncovalent interaction area with the naphthyl group of ligand **F**, while the isopropyl group is rotated outwards and does not interact with the **F** ligand (Figure 2A). Considerable differences between the matched and mismatched cases, especially for the ligands **E**/**E′** and **H**/**H′**, show that a stable conformation in the mismatched case provides a considerably better interface compared to the matched one (see Table 1 and SI Chapter 6.1).[45]

This example illustrates that the Ph(Me)CH group is engaged in strong interactions with the naphthyl ring as the key interaction for the heterocomplex preference. The interaction of the Ph(Me)CH group with the biphenol in the homocomplex *cis*-Pd(**E**)$_2$$Cl_2$ must be thus weaker and responsible for the heterocomplex preference (see blue and red circle in Figure 2A).[46] The presence of the aryl ring, methyl group and polarization of the methine C–H bond make this group an extremely interesting dispersion energy donor in catalysis, especially in combination with extended, rigid naphthyl ring. Therefore, this conformation was used to calibrate computational methods and to analyze these interactions in detail.

Table 1: Preference of heterocomplex formation upon alkyl group variation in ligand **A** or **A′** (matched and mismatched regarding **F**). Given are the *cis*-Pd(**E**)(**F**)Cl_2/*cis*-Pd(**E**)$_2$$Cl_2$/*cis*-Pd(**F**)$_2$$Cl_2$ ratios.[a]

Ligand X	(X)(**F**):(X)$_2$:(**F**)$_2$	Ligand X	(X)(**F**):(X)$_2$:(**F**)$_2$
A1 (Ph(Me)CH)	2.2:1.0:1.1	**D** (Bn)	3.5:1.0:1.0
A1′ (Ph(Me)CH)	4.4:1.0:0.9	**D′** (Bn)	3.2:0.9:1.0
A2 (Naphth(Me)CH)	2.3:1.0:1.0	**E** (*i*-Pr)	8.0:1.0:1.0
A2′ (Naphth(Me)CH)	1.6:1.0:1.1	**E′** (*i*-Pr)	22.0:0.9:1.0
B (Me)	1.0:1.0:1.0	**G** ($C_6F_5CH_2$)	3.0:1.2:1.0
B′ (Me)	1.2:1.0:0.7	**G′** ($C_6F_5CH_2$)	6.2:1.0:1.0
C (Et)	1.7:1.0:1.0	**H** (Cy)	3.0:0.6:1.0
		H′ (Cy)	15.0:0.6:1.0

[a] Ratio determined by $^{31}P\{^1H\}$ NMR, CD_2Cl_2, 300 K.

Computational Investigations: Conformational Space and Noncovalent Interactions

To provide reasonable 3D structures of the complexes that could be later narrowed down based on their energetics and NOE constraints, we generated 500 conformers for each *cis*-Pd(**E**)(**F**)Cl_2 and *cis*-Pd(**E′**)(**F**)Cl_2 complexes, as well ≈170 conformers of the corresponding homocomplexes by GFN2-xTB metadynamics.[47] All the structures were optimized at PBE-D3(BJ)/def2-SVP/CPCM(CH_2Cl_2)[48] level of theory using Orca computational software.[49] The conformers with DFT energies < 20 kJ mol^{-1} were considered further and their

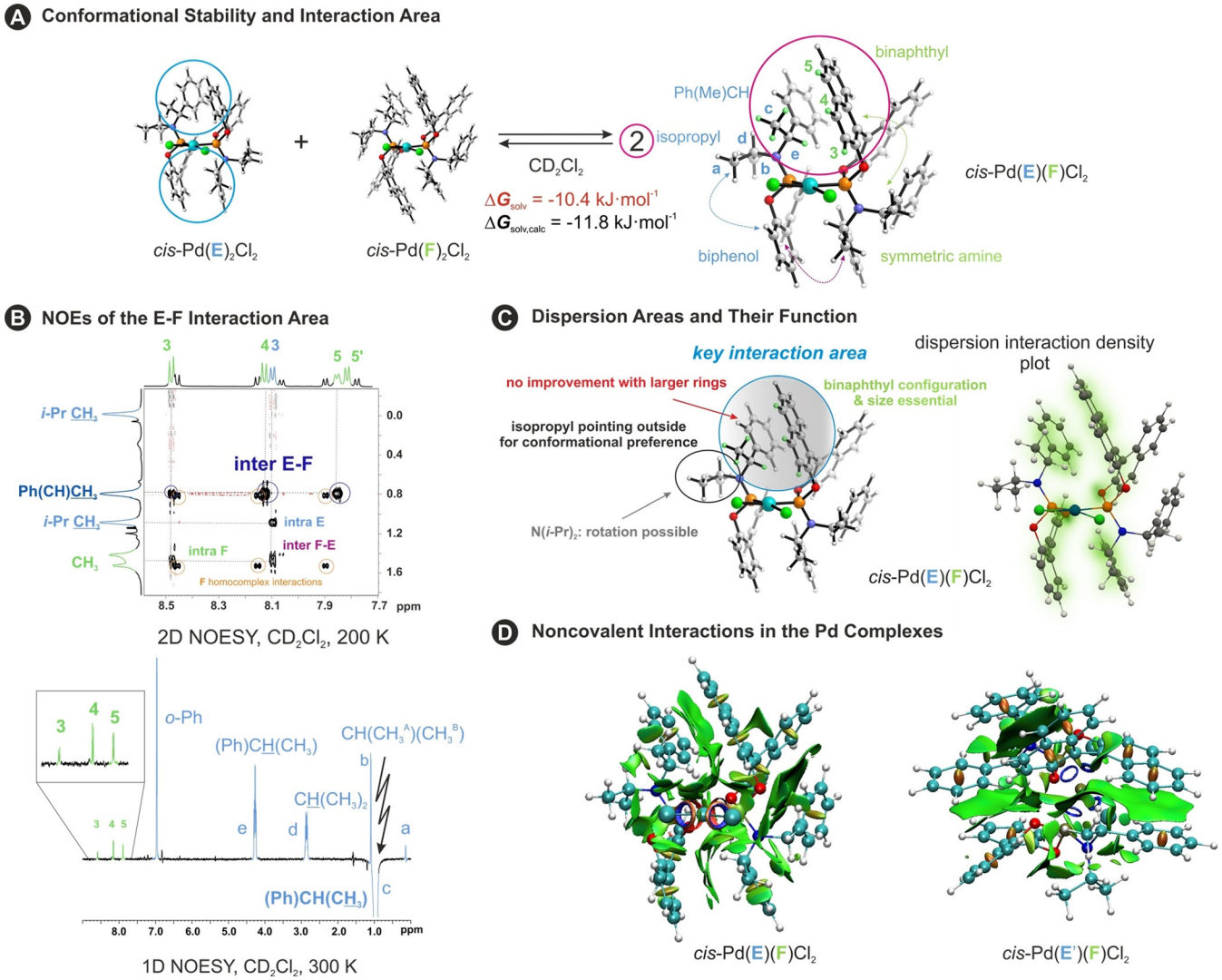

Figure 2. a) Structures of the homocomplexes and the heterocomplex *cis*-Pd(**E**)(**F**)Cl_2 in CD_2Cl_2, the interligand interaction areas are highlighted. The preferred formation of the heterocomplex is reproduced by calculations in terms of ΔG_{solv} (B2PLYP/CBS(TQ)/SMD(CH_2Cl_2)//PBE-D3(BJ)/def2-SVP/CPCM(CH_2Cl_2). b) 1D and 2D NOESY data reveal a close proximity of the Ph(Me)CH group and the binaphthyl core and define interligand interactions. c) Key interaction area in the stabilized heterocomplexes with functional features for its preference. Dispersion interaction density plot (DLPNO-CCSD(T)/def2-TZVP) shows a major role of dispersion in the interactions. d) NCI plots of *cis*-Pd(**E**)(**F**)Cl_2 and *cis*-Pd(**E'**)(**F**)Cl_2 showing a larger, continuous dispersion area in the mismatched complex.

Gibbs free energies were calculated based on B2PLYP/CBS single-point energies[50] with solvation and Gibbs free energy corrections (see SI).[51,52]

For all the hetero- and homocomplexes one lowest energy structure was found, which also fits to the NOE contacts—solvent-exposed isopropyl group is oriented out of the complex (Figure 2A). Other orientations of the amine side chain of *cis*-Pd(**E**)(**F**)Cl_2 could be excluded based on both NOE data and computed energetics (see SI Chapter 12.5.1). Additionally, ^{13}C NMR chemical shifts were computed at TPSS/IGLO-III/SMD(CH_2Cl_2), and indeed, the lowest energy structure correlated best with the experiment data.

B2PLYP/CBS(TQ)-based Gibbs energies without D3 correction predict correct ΔG for the equilibrium of *cis*-Pd(**E**)(**F**)Cl_2 and the corresponding homocomplexes (exp. $-10.4\ kJ\,mol^{-1}$; calc. $-11.8\ kJ\,mol^{-1}$ in favor of the heterocomplex). However, the subtle differences in the diastereomeric heterocomplex preference of *cis*-Pd(**E'**)(**F**)Cl_2 were not completely picked up by the computations and slightly lower equilibrium ΔG was predicted (exp. $-15.7\ kJ\,mol^{-1}$; calc. $-6.0\ kJ\,mol^{-1}$). When the D3 correction was employed, the preference between the homo- and heterocomplexes switched, contrary to the experiments. The fact that the approach without the D3 correction resulted in better reproduction of the energies was reported previously in some solvated systems.[53,54]

Additionally, large noncovalent interactions areas were revealed in an NCI plot (Figure 2C).[55] An especially large continuous area could be recognized in the *cis*-Pd(**E'**)(**F**)Cl_2 complex and therefore a large dispersion contribution is expected. To quantify the dispersion contribution to the stability of the complexes, we conducted local energy

decomposition[56,57] at DLPNO-CCSD(T)/def2-TZVP level of theory.[58] Thus, interligand London dispersion interaction in *cis*-Pd(**E**)(**F**)Cl_2 was calculated to be −129 kJ mol^{-1}, comparable to the interligand electrostatic interaction (−95 kJ mol^{-1}), as well as a considerable dispersion contribution in the dative Pd–P bonds (−80 kJ mol^{-1} for each ligand). Surprisingly, the dispersion interaction in *cis*-Pd(**E′**)(**F**)Cl_2 was about the same (see SI Chapter 12.7). Similar magnitude of London dispersion and electrostatics (including dipole–dipole interactions) suggests that both factors contribute to the preference of the heterocomplexes. Thus, in the following step, the electrostatics and dispersion areas were varied and their impact on the heterocomplex preferences was investigated experimentally.

Aryl–Aryl Interactions in the Interligand Interaction Area

Now, having at hand both the stable conformation of the TM complex and the analysis of the key interligand interaction area, we tuned its electronic and steric properties and analyzed the outcome on the heterocomplex preference (Figure 3A). Moreover, this allows to evaluate the $\Delta\Delta G$ values of the balance, which reflect the different orientation of the matched and mismatched ligand inside the interaction area of the heterocomplex. In addition, we explored the stability of the heterocomplexes in different solvents.

First, we synthesized different ligands to achieve electronic variation. Ligands **E2**/**E2′** and **E3**/**E3′** contain an electron-donating methoxy group in *para* or *meta* position, while ligands **E4**/**E4′** have an electron-withdrawing fluorine atom in the *para* position (Figure 3A). Next, we interpreted the preferences of the heterocomplexes within the matched structures (see interactions to biphenol and binaphthol in Figure 2A). The methoxy groups in both positions slightly increased the ratio from 8:1:1 to 11:1:1 ((*R*)-Alexakis ligand with matched stereochemistry to **F**; see hetero- to homocomplex ratios in Table 2). In the case of **E4**, the electron-withdrawing effect of fluorine decreased the ratio slightly. The same effect of fluorine substituent was reported by Cockroft et al.[54] Chemical shift analysis revealed that this electronic variation does not affect the aliphatic C–H bond polarization, thus mainly aryl–naphthyl interactions (including dipole–dipole interactions) are optimized.

In the mismatched cases, the aryl and naphthyl groups are not only closer in space but interacting more strongly as evidenced from the $\Delta\Delta G$ values which are in favor of the mismatched structures (Figure 3B). This should allow for more pronounced modulation and indeed, the highest effect is found for the methoxy group with **E2′** (increase from 22:1:1 to 29:1:1), while fluorine in the mismatched case **E4′** had the same effect as hydrogen in **E′**. Interestingly, the $\Delta\Delta G$ values of **E**, **E2** and **E4** series (5.3–6.3 kJ mol^{-1}, Table 2) are similar, suggesting the same change of interactions for both matched and mismatched cases.

Next, the steric effects were investigated. Introduction of naphthyl substituents either in 1- or 2- positions (ligands **E5**/**E5′** and **E6**/**E6′**) led to a decrease in the heterocomplex populations. Especially ligand **E6′** cannot develop the specific

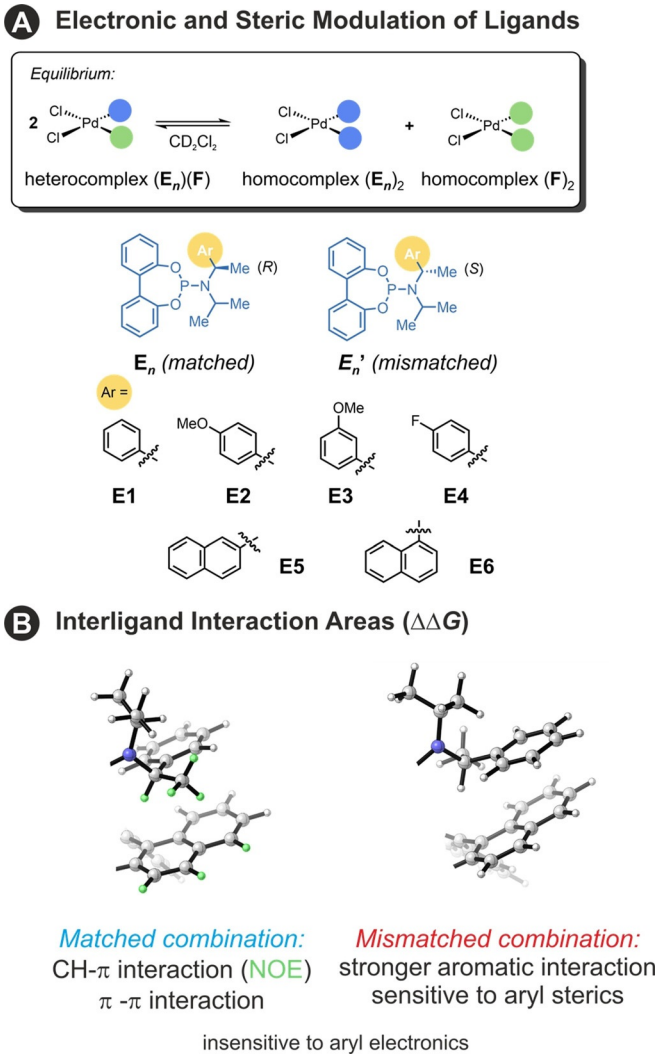

Figure 3. a) Equilibrium between the hetero- and homocomplexes; ligand structures with the electronic and steric variations of the ligand aryl substituent. b) Interligand interaction areas in the matched and mismatched ligand combinations. Higher preference for the heterocomplex in the mismatched case is due to stronger aromatic interactions.

Table 2: Equilibrium complex ratios in CD_2Cl_2 upon ligand aryl group variations.

Ligand E_n/E'_n	(X)(**F**):$(X)_2$:$(F)_2$ (matched)	(X′)(**F**):$(X')_2$:$(F)_2$ (mismatched)	$\Delta\Delta G$[b,c] [kJ mol^{-1}]
E_1 = E	8.0:1.0:1.0	22.0:0.9:1.0	5.3
	12.0:1.0:1.0	64.0:1.0:1.0[d]	8.4
E_2	11.6:1.5:1.0	29.0:1.0:1.0[b]	5.6
E_3	11.0:1.0:0.8	3.0:1.0:1.2	−7.5
E_4	6.0:1.0:1.0	21.0:1.0:1.0	6.3
E_5	6.3:1.0:1.0	16.0:1.0:1.0	4.7
E_6	6.8:1.0:1.0	broad peaks	–

[a] Ratio determined by $^{31}P\{^1H\}$ NMR (151 MHz), CD_2Cl_2, 300 K. [b] Other $(E)_2$ homocomplexes were present. [c] $\Delta\Delta G$ was calculated as the difference between ΔG of the matched and mismatched equilibrium, assuming that the concentration of *cis*-Pd$(X)_2Cl_2$ is equal to *cis*-Pd$(F)_2Cl_2$, irrespective of other **X** homocomplexes present. [d] In $CDCl_3$.

favorable conformation as indicated by broad peaks in ^{1}H and ^{31}P NMR spectra. A substantial reduction of heterocomplex preference was observed in the case of *meta*-substituted ligand **E3′** with inversion of the matched/mismatched preference ($\Delta\Delta G$ −7.5 kJ mol^{-1}). A similar decrease of the heterocomplex formation was observed when employing symmetric ligands **A2**/**A2′** with two naphthyl rings (Figure 1C and Table 1). Thus, in these cases, the more rigid structure of both parts of the interaction area seems to reintroduce the classical repulsion penalty of steric hindrance.

Finally, to investigate the influence of the solvent on the equilibria, we examined the stability of the heterocomplexes *cis*-Pd(**E**)(**F**)Cl_2 and *cis*-Pd(**E′**)(**F**)Cl_2 in three solvents (CD_2Cl_2, $CDCl_3$ and [D_8]toluene) with different dielectric constants/polarizabilities (ε_r 8.93–2.38). The enhancement of interactions in less polar solvents were reported, for example, in an anion recognition system.[59,60] Solvents such as [D_8]THF showed coordination to the metal ion. The bias towards the heterocomplex was preserved in all the investigated solvents (see SI Chapter 7.5). In $CDCl_3$, the preference for the *cis*-Pd(**E′**)(**F**)Cl_2 increased to 64:1:1 compared to 22:1:1 in CD_2Cl_2. Since exchange of interligand interactions dominates the preference, in the first assumption solvophobic effects and solvent–solvent interactions should not play a role. Thus, this increased preference can be interpreted as a strengthening of the van der Waals forces and electrostatics (dipole–dipole, induction, and dispersion) of ligand–ligand interactions in less polar solvents.

Thus, these data show that the combination of conformational stability, interaction optimization and solvent can lead to high heterocomplex preferences.

Conclusion

In summary, we have shown that the preference for Pd bis(phosphoramidite) heterocomplexes can be achieved by substituent variations of the highly flexible biphenol phosphoramidite ligands. This preference is in line with the conformational stability of the complexes.

Specifically, high populations of the heterocomplexes containing two different ligands, which are useful in asymmetric catalysis owing to their higher activity or selectivity, could be achieved when nonsymmetric biphenol ligands with branched alkyl groups were employed. Therefore, both the structural and populational preferences can be the result of intramolecular interligand dispersion interactions. The potential interaction areas of the ligands were shown by NMR analysis of NOE contacts and chemical shift dispersion. To identify potential structures which corroborate the NMR data, screening of a large number of conformers by computational methods was performed, and revealed the 3D structures of the complexes. The examined system shows that all van der Waals interactions and electrostatics (dipole–dipole, induction and dispersion) play a role in the stability and structural preference of the complexes, as proposed by the direct interaction model, that is, the relative position and orientation of the aryl rings is decisive.[61–63] Additionally, solvent polarity can influence the position of the equilibria but not the absolute preference of the heterocomplexes.

We have shown that the enthalpic stabilization by attractive noncovalent interactions translates into the high heterocomplex preferences. Overall, conformational stability is enhanced by the enthalpic contribution from the combination of extended, rigid structures with flexible counterpart (methyl or phenyl groups).

This interaction pattern can be relayed to catalysis, where it is usually not feasible to gain structural information directly, e.g., due to equilibria in copper-catalyzed reactions.[27] We are confident that the interligand interactions of the designed, nonsymmetric phosphoramidite ligands could be transferred and applied to the interactions of the ligand with the substrate. An encouraging result that confirms our point came via different approach from the ligand screening in a Cu-catalyzed reaction, which exploits the nonsymmetric phosphoramidite ligands having both aromatic and branched aliphatic substituents.[30,31] These serve as extended interactions areas, similar to those identified in this study. We believe that our results, which are based on ligands and complexes highly relevant in catalysis, have the potential to be used as a design principle for modelling ligand–ligand or ligand–substrate interactions independent of the transition metal employed, or as a ligand screening tool in catalysis. We hope the results presented here would aid researchers in designing and synthesizing molecules with desired properties, e.g., binding or folding.

Acknowledgements

Financial and intellectual support was provided by the DFG (SPP 1807 Control of London dispersion interactions in molecular chemistry) and the European Research Council (ERC-CoG 614182—IonPairsAtCatalysis). We thank Pavel Shelyganov for assistance with some experiments and Adam Sikorják for manuscript proofreading. Open Access funding enabled and organized by Projekt DEAL.

Conflict of Interest

The authors declare no conflict of interest.

Keywords: conformational analysis · NMR spectroscopy · noncovalent interactions · phosphoramidites · supramolecular balance

[1] J. P. Wagner, P. R. Schreiner, *Angew. Chem. Int. Ed.* **2015**, *54*, 12274 – 12296; *Angew. Chem.* **2015**, *127*, 12446 – 12471.
[2] E. H. Krenske, K. N. Houk, *Acc. Chem. Res.* **2013**, *46*, 979 – 989.
[3] A. Armstrong, R. A. Boto, P. Dingwall, J. Contreras-García, M. J. Harvey, N. J. Mason, H. S. Rzepa, *Chem. Sci.* **2014**, *5*, 2057 – 2071.
[4] S. E. Wheeler, T. J. Seguin, Y. Guan, A. C. Doney, *Acc. Chem. Res.* **2016**, *49*, 1061 – 1069.
[5] A. J. Neel, M. J. Hilton, M. S. Sigman, F. D. Toste, *Nature* **2017**, *543*, 637 – 646.

[6] D. Yepes, F. Neese, B. List, G. Bistoni, *J. Am. Chem. Soc.* **2020**, *142*, 3613 – 3625.
[7] B. Pölloth, M. P. Sibi, H. Zipse, *Angew. Chem. Int. Ed.* **2021**, *60*, 774 – 778; *Angew. Chem.* **2021**, *133*, 786 – 791.
[8] C. Eschmann, L. Song, P. R. Schreiner, *Angew. Chem. Int. Ed.* **2021**, *60*, 4823 – 4832; *Angew. Chem.* **2021**, *133*, 4873 – 4882.
[9] S. Paliwal, S. Geib, C. S. Wilcox, *J. Am. Chem. Soc.* **1994**, *116*, 4497 – 4498.
[10] E. I. Kim, S. Paliwal, C. S. Wilcox, *J. Am. Chem. Soc.* **1998**, *120*, 11192 – 11193.
[11] S. L. Cockroft, C. A. Hunter, *Chem. Commun.* **2006**, 3806 – 3808.
[12] S. L. Cockroft, C. A. Hunter, *Chem. Soc. Rev.* **2007**, *36*, 172 – 188.
[13] I. K. Mati, S. L. Cockroft, *Chem. Soc. Rev.* **2010**, *39*, 4195 – 4205.
[14] M. A. Strauss, H. A. Wegner, *Angew. Chem. Int. Ed.* **2019**, *58*, 18552 – 18556; *Angew. Chem.* **2019**, *131*, 18724 – 18729.
[15] G. Platzer, M. Mayer, A. Beier, S. Brüschweiler, J. E. Fuchs, H. Engelhardt, L. Geist, G. Bader, J. Schörghuber, R. Lichtenecker, et al., *Angew. Chem. Int. Ed.* **2020**, *59*, 14861 – 14868; *Angew. Chem.* **2020**, *132*, 14971 – 14978.
[16] Q. Lu, F. Neese, G. Bistoni, *Phys. Chem. Chem. Phys.* **2019**, *21*, 11569 – 11577.
[17] S. Singha, M. Buchsteiner, G. Bistoni, R. Goddard, A. Fürstner, *J. Am. Chem. Soc.* **2021**, *143*, 5666 – 5673.
[18] C. B. Santiago, J. Y. Guo, M. S. Sigman, *Chem. Sci.* **2018**, *9*, 2398 – 2412.
[19] J. F. Teichert, B. L. Feringa, *Angew. Chem. Int. Ed.* **2010**, *49*, 2486 – 2528; *Angew. Chem.* **2010**, *122*, 2538 – 2582.
[20] M. Žabka, R. Šebesta in *Chiral Lewis Acids in Organic Synthesis* (Ed. J. Mlynarski), Wiley-VCH, Weinheim, **2017**, pp. 223 – 260.
[21] A. H. M. de Vries, A. Meetsma, B. L. Feringa, *Angew. Chem. Int. Ed. Engl.* **1996**, *35*, 2374 – 2376; *Angew. Chem.* **1996**, *108*, 2526 – 2528.
[22] A. J. Minnaard, B. L. Feringa, L. Lefort, J. G. de Vries, *Acc. Chem. Res.* **2007**, *40*, 1267 – 1277.
[23] A. Alexakis, S. Rosset, J. Allamand, S. March, F. Guillen, C. Benhaim, *Synlett* **2001**, 1375 – 1378.
[24] A. Alexakis, C. Benhaim, *Eur. J. Org. Chem.* **2002**, 3221 – 3236.
[25] A. Alexakis, D. Polet, S. Rosset, S. March, *J. Org. Chem.* **2004**, *69*, 5660 – 5667.
[26] I. S. Mikhel, G. Bernardinelli, A. Alexakis, *Inorg. Chim. Acta* **2006**, *359*, 1826 – 1836.
[27] K. Schober, E. Hartmann, H. Zhang, R. M. Gschwind, *Angew. Chem. Int. Ed.* **2010**, *49*, 2794 – 2797; *Angew. Chem.* **2010**, *122*, 2855 – 2859.
[28] E. Hartmann, M. M. Hammer, R. M. Gschwind, *Chem. Eur. J.* **2013**, *19*, 10551 – 10562.
[29] R. N. Straker, Q. Peng, A. Mekareeya, R. S. Paton, E. A. Anderson, *Nat. Commun.* **2016**, *7*, 10109.
[30] R. Ardkhean, P. M. C. Roth, R. M. Maksymowicz, A. Curran, Q. Peng, R. S. Paton, S. P. Fletcher, *ACS Catal.* **2017**, *7*, 6729 – 6737.
[31] A. V. Brethomé, R. S. Paton, S. P. Fletcher, *ACS Catal.* **2019**, *9*, 7179 – 7187.
[32] E. Hartmann, R. M. Gschwind, *Angew. Chem. Int. Ed.* **2013**, *52*, 2350 – 2354; *Angew. Chem.* **2013**, *125*, 2406 – 2410.
[33] M. T. Reetz, G. Mehler, *Tetrahedron Lett.* **2003**, *44*, 4593 – 4596.
[34] M. T. Reetz, T. Sell, A. Meiswinkel, G. Mehler, *Angew. Chem. Int. Ed.* **2003**, *42*, 790 – 793; *Angew. Chem.* **2003**, *115*, 814 – 817.
[35] D. Peña, A. J. Minnaard, J. A. F. Boogers, A. H. M. De Vries, J. De Vries, B. L. Feringa, *Org. Biomol. Chem.* **2003**, *1*, 1087 – 1089.
[36] A. Duursma, R. Hoen, J. Schuppan, R. Hulst, A. J. Minnaard, B. L. Feringa, *Org. Lett.* **2003**, *5*, 3111 – 3113.
[37] B. Breit, *Angew. Chem. Int. Ed.* **2005**, *44*, 6816 – 6825; *Angew. Chem.* **2005**, *117*, 6976 – 6986.
[38] C. Monti, C. Gennari, U. Piarulli, *Chem. Eur. J.* **2007**, *13*, 1547 – 1558.
[39] Y. Fan, M. Cong, L. Peng, *Chem. Eur. J.* **2014**, *20*, 2698 – 2702.
[40] W. Fu, W. Tang, *ACS Catal.* **2016**, *6*, 4814 – 4858.
[41] M. Chen, X. Wang, P. Yang, X. Kou, Z. H. Ren, Z. H. Guan, *Angew. Chem. Int. Ed.* **2020**, *59*, 12199 – 12205; *Angew. Chem.* **2020**, *132*, 12297 – 12303.
[42] O. Pàmies, J. Margalef, S. Cañellas, J. James, E. Judge, P. J. Guiry, C. Moberg, J. E. Bäckvall, A. Pfaltz, M. A. Pericàs, et al., *Chem. Rev.* **2021**, *121*, 4373 – 4505.
[43] I. S. Mikhel, K. N. Gavrilov, A. I. Polosukhin, A. I. Rebrov, *Russ. Chem. Bull.* **1998**, *47*, 1585 – 1588.
[44] S. Filipuzzi, P. S. Pregosin, A. Albinati, S. Rizzato, *Organometallics* **2006**, *25*, 5955 – 5964.
[45] Rotational barriers seem not to be important for the system, because the introduction of two isopropyl groups to the ligand nitrogen resulted in a slow interchange at 190 K, suggesting quite low kinetic barrier (see SI Chapter 6.2).
[46] There are two interligand interaction areas in the **E** homocomplex and one key interligand interaction area in two molecules of the heterocomplex. The **F** homocomplex interaction areas remain the same in all the equilibria.
[47] S. Grimme, *J. Chem. Theory Comput.* **2019**, *15*, 2847 – 2862.
[48] J. P. Perdew, K. Burke, M. Ernzerhof, *Phys. Rev. Lett.* **1996**, *77*, 3865 – 3868.
[49] F. Neese, *Wiley Interdiscip. Rev.: Comput. Mol. Sci.* **2018**, *8*, 4 – 9.
[50] S. Grimme, *J. Chem. Phys.* **2006**, *124*, 034108.
[51] S. Grimme, *Chem. Eur. J.* **2012**, *18*, 9955 – 9964.
[52] B. Schirmer, S. Grimme in *Frustrated Lewis Pairs I* (Eds.: G. Erker, D. W. Stephan), Springer, Heidelberg, **2013**, pp. 213 – 230.
[53] L. Yang, C. Adam, G. S. Nichol, S. L. Cockroft, *Nat. Chem.* **2013**, *5*, 1006 – 1010.
[54] L. Yang, J. B. Brazier, T. A. Hubbard, D. M. Rogers, S. L. Cockroft, *Angew. Chem. Int. Ed.* **2016**, *55*, 912 – 916; *Angew. Chem.* **2016**, *128*, 924 – 928.
[55] E. R. Johnson, S. Keinan, P. Mori-Sánchez, J. Contreras-García, A. J. Cohen, W. Yang, *J. Am. Chem. Soc.* **2010**, *132*, 6498 – 6506.
[56] W. B. Schneider, G. Bistoni, M. Sparta, M. Saitow, C. Riplinger, A. A. Auer, F. Neese, *J. Chem. Theory Comput.* **2016**, *12*, 4778 – 4792.
[57] G. Bistoni, *Wiley Interdiscip. Rev.: Comput. Mol. Sci.* **2020**, *10*, e1442.
[58] C. Riplinger, B. Sandhoefer, A. Hansen, F. Neese, *J. Chem. Phys.* **2013**, *139*, 134101.
[59] S. L. Cockroft, *Chem* **2017**, *3*, 383 – 384.
[60] Y. Liu, A. Sengupta, K. Raghavachari, A. H. Flood, *Chem* **2017**, *3*, 411 – 427.
[61] S. E. Wheeler, *J. Am. Chem. Soc.* **2011**, *133*, 10262 – 10274.
[62] S. E. Wheeler, *Acc. Chem. Res.* **2013**, *46*, 1029 – 1038.
[63] D. E. Fagnani, A. Sotuyo, R. K. Castellano in *Comprehensive Supramolecular Chemistry II* (Ed. J. L. Atwood), Elsevier, Oxford, **2017**, pp. 121 – 148.

Manuscript received: May 23, 2021
Accepted manuscript online: September 29, 2021
Version of record online: November 2, 2021

